Geophysical Modelling of the Middle America Trench using GMT

Polina Lemenkova

Annals of Valahia University of Targoviste. Geographical Series (2019), **19**(2): 73-94
DOI: 10.2478/avutgs-2019-0008
ISSN (Print): 2393-1485, ISSN (Online): 2393-1493

GEOPHYSICAL MODELLING OF THE MIDDLE AMERICA TRENCH USING GMT

Polina LEMENKOVA
Ocean University of China, College of Marine Geo-sciences. 238 Songling Rd. Laoshan, 266100, Qingdao, Shandong, PRC. Tel.: +86-1768-554-1605. email: pauline.lemenkova@gmail.com

Abstract

The study is focused on the geomorphological analysis of the Guatemala Trench, East Pacific Ocean. Research goal is to find geometric variations in western and eastern flanks of the trench and correlation of the submarine geomorphology with geologic settings and seismicity through numerical and graphical modelling. Methods include GMT based analysis of the bathymetry, geomorphic shape and surface trends in topography and gravity grids. Dataset contains raster grids on bathymetry, gravity, geoid and geological layers. Technical workflow is following: 1) Bathymetric mapping by modules ('grdcut', 'grdimage'); 2) Datasets visualizing and analysis, 3) Topographic and gravimetric surface modelling by ASCII data; 4) Cartographic mapping ('psbasemap', 'psxy', 'grdcontour') 4) 3D-mesh modelling; 5) Automatically digitized orthogonal cross-stacked profiles ('grdtrack'); 6) Visualizing curvature trends ('trend1d'); 7) statistical histograms. Results reveal unevenness in the structure of the submarine landforms. Modelling cross-section profiles highlighted depth variation at different parts of the transects and seafloor segments. Geomorphic structure has straight shape form of the slopes with steep oceanward forearc. Its geometry has steep and strait shape which correlates with seismicity. Depth samples vary: -3000 to -6200 m, seafloor is 3-5 km wide. Trench has symmetric accurate 'V-shaped' geometric form for the segment of -30 to -30 km. Oceanward side slope increases towards continental shelf, left flank stabilizes in depths at -50 km from the trench axis, deepens at -50 to 0 m, decreases at -3,200 to -5,800. Oceanward flank gradient varies: slope steepness of 35,63° at 0-20 km, 42,17° at 20-40 km, 44° at 40-60km. Left flank has 43,24° at 0-24 km, 28,33° at 24-40 km, 14° at 40-60 km, 1,13° at 60-200 km. Marine vertical gravity correlates with tectonic slab contours (20-30 mGal on the trench slopes). The study demonstrated effective GMT-based framework with a multi-disciplinary scope that combined cartographic methods of modelling deep-sea trench profiles with geological, bathymetric and geophysical analysis. Technical application of the advanced cartographic solutions and high quality mapping by GMT demonstrated its functionality for data analysis and effectiveness of the geoinformation processing. Proposed techniques and workflow methodology provided framework for geological mapping and can be applied in further similar research.
Keywords: GMT; data analysis; bash script; oceanic trench; geomorphology; Pacific Ocean; geology

1 INTRODUCTION

The general form of the submarine geomorphology and the presence of the oceanic deep-sea trenches in the margins of the Pacific Ocean have been known and studied in 20 century (Shepard, 1963). However, despite more detailed data on the structure of the oceanic trenches (Heezen and Tharp 1977), only recently with a progress in quantitative GIS has precise ocean mapping become available (Becker et al 2009, Amante and Eakins 2009). Development of the global DEM grids covering Earth surface and satellite altimeter-derived precise high-resolution topography (Smith 1993, Smith and Sandwell 1997b) initiated a step forward in seafloor mapping (Gauger et al 2007; Lemenkova 2019h). This has been improved by combining bathymetric data with other geospatial datasets to create global grids, e.g. SRTM_15PLUS, or GEBCO 30 arc sec covering global seafloor.

Ocean geomorphology, origin of the formation and types of the submarine landforms were constantly arising interest throughout the 20th century until now. Understanding a variety of the submarine landforms hidden from the human eyes due to their remote location, and factors affecting seafloor geomorphology is a very complex task that requires a multi-disciplinary approach: geological data analysis, data processing and modelling by advanced algorithms, geostatistical analysis and visualization (Lemenkova 2019g). Rapid development of the IT technologies in XXI century enabled to perform stream data processing which contributes to our better understanding of the marine geomorphology. Attempt of the seafloor mapping and monitoring exist (Lanier et al 2007; Monahan 2004) and the advances in marine seafloor mapping are developing. Mapping geomorphology of the oceanic trenches aims at highlighting specific shapes of their unique landforms. Significance and importance of the ocean seafloor mapping can be summarized through target key components: ecosystem management; observations of the marine habitats (fish, benthos); updating global topographic datasets; economic monitoring and evaluation of the seabed natural marine resources.

Geoinformation is fundamental for understanding ocean seafloor and precise bathymetric mapping. Combining detailed datasets of the seafloor raster maps with geomorphic modelling can increase our knowledge of the seafloor variability and factors affecting seafloor landforms. Geomorphology of the deep-sea trenches is mainly controlled by eight variables: tectonic plates movements, seismicity and volcanism directly affecting sedimentation, sediment size, and load intensity, gradient and depth of the slopes, ocean currents velocity contributing to the sedimentation.

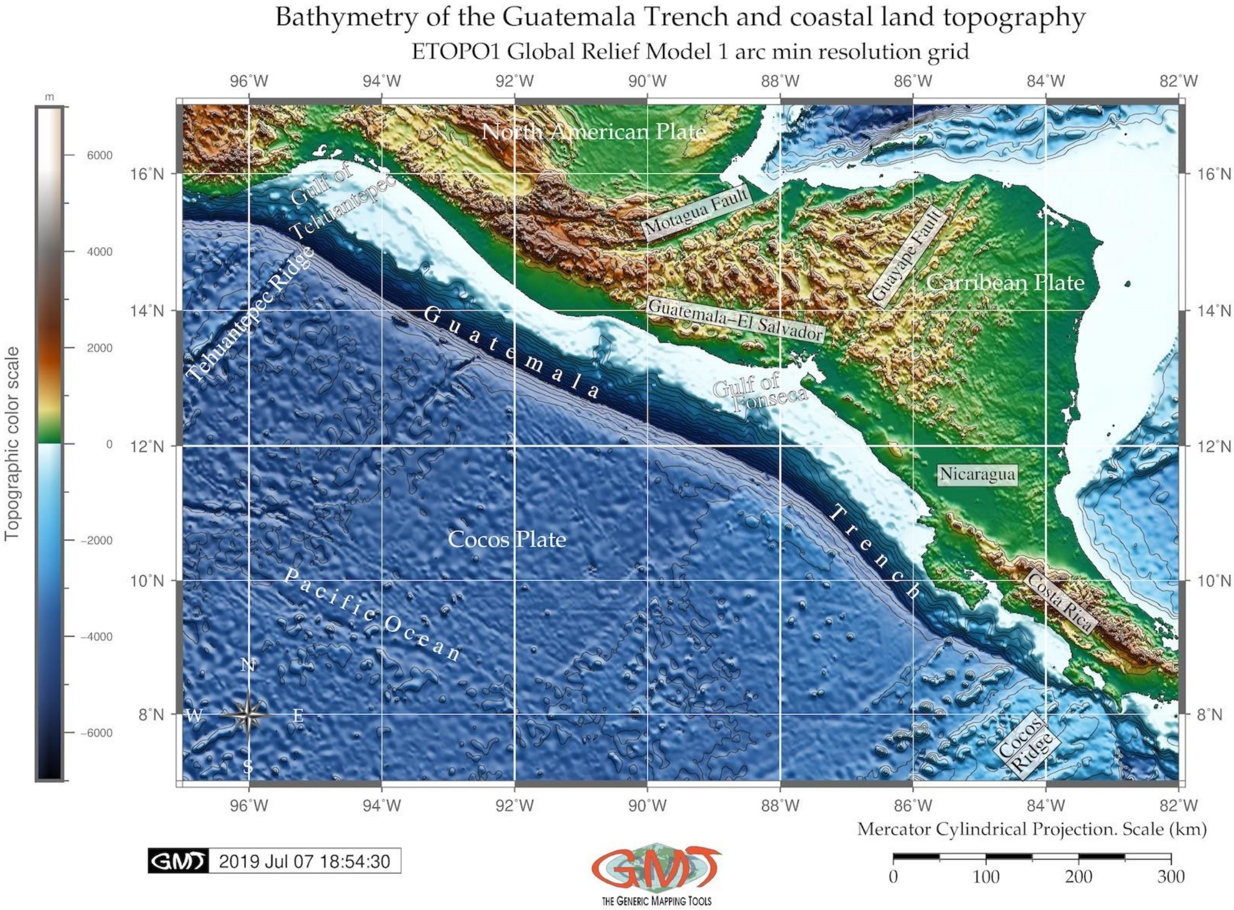

Figure 1. Bathymetry of the Guatemala Trench. Cartographic base data: ETOPO1.

A specifics of the marine geologic datasets consists in traditionally large volumes of the sampling observations derived from the cruises, along with their variety and different types (e.g., lithology and rocks of the seafloor, geological structure, tectonics etc). Using such multi-source variables requires advanced methods for data processing. The advantages of the modern cartographic technologies applied for marine geology, such as GMT shell scripting, include increased precision of the data processing and quality of the cartographic output.

Moreover, combination of the advanced methods of scripting GMT approach with thorough data analysis on geologic and tectonic settings of the study area enables to better understand hidden correlation between the current land format and historical development (e.g. closeness of ridges, stretch of lineaments, faults, distribution of the seismic zones in relation with the study area). Finally, the speed of the data processing by GMT shell scripting, comparing, for instance, with traditional manual digitizing, enables to generate new datasets for reprocessing with target coordinates, which is indisputably actual for the marine geologic research.

In view of these reasons, the advantages of using GMT for modelling and mapping ocean trench provides clear perspectives. Specifically designed modules of GMT are focused don visualizing target objects (e.g. lineament by 'psxy', general cartographic elements by 'psbasemap', isolines by 'grdcontour', etc.). This enables to use such approach as a 'layer-based' hierarchical GIS philosophy to extract the insights in the complexity of the marine geological objects, factors and phenomena constituting the structure of the submarine seafloor, which is demonstrated in the shell scripts of the current work.

Target aim of the presented research is visualizing, numerical and graphical modelling of the submarine geomorphology of the Guatemala Trench, Figure 1. Research methodology is based on the geospatial and statistical analysis using Generic Mapping Tools (GMT) modules. The specific focus of this work is laid on its multi-disciplinary scope that combines cartographic methods of the geospatial and statistical data modelling by GMT with analysis of the general setting of the study area: geological, bathymetric and geophysical properties. Methodologically, the research included data visualization, modelling cross-section profiles and mapping, statistical analysis of the submarine landforms of the trench. The initial geo data were extracted from the USGS public sources as well as available embedded layers in the GMT (e.g. coastlines).

The novelty of the research described and presented in this paper is associated with the progress in geoinformation technologies applied for geological mapping and geomorphic analysis. Having access to the machine learning technologies associated with rapid recent IT progress (scripting coding, high-resolution datasets and DEMs), approach of data analysis offered by GMT can be employed for marine geological research to provide new, more detailed insight into the seafloor bathymetry. GMT modules enable to perform a speed but quality map-making and data processing based on the high-resolution DEMs. In turn, this allows to study in details submarine geomorphic objects and the associated landforms of the oceanic seafloor.

2 STUDY AREA

Middle America Trench is unique among other Pacific trenches, since its nature is complex and varies in its different parts. It consists of two distinct parts with varying features of the oceanic plate and geology in either: northern and southern. Guatemala Trench presents a southern part of the Middle America Trench, a hadal trench trending northwest (Figure 3), which marks the Caribbean-Cocos plate boundary in the east Pacific Ocean (Guzman et al 2006). The division between the both parts goes by the Tehuantepec Ridge, a linear undersea ridge located off the west coast of Mexico in the Pacific Ocean, a remnant of an old fracture zone formed as a fracture zone and transform fault along the East Pacific Rise that reoriented the fracture zone as a result of a change in the motion of the Pacific Plate (Turcotte and Schubert 2013).

Northern part of the Middle America Trench, located off Mexico, sometimes referred to as Acapulco Trench, was initiated by a large slip motion giving to the Honduras Platform an offset of ca. 800 km and cutting off Mexican structure. It is a small hadal trench, a part of the East Pacific Rise stretching from from Jalisco to Tehuantepec Ridge. Here, the Middle America Trench goes along the North American continent along Mexico up to the Guatemala Transverse Zone. Middle America Trench runs very obliquely, and hence, not related to the neotectonic features of Mexico.

Its southern part, the Guatemala Trench, is resulted from a subduction zone related to the Franciscan subduction zone of North America where the Isthmus of Panama supports a huge Tertiary volcanic cover. Here Guatemala Trench originated from an ancient subduction zone involving Mesozoic oceanic sediments and crust (Aubouin et al 1982). Located on the Cocos tectonic plate, Guatemala Trench stretches between the Tehuantepec and Cocos Ridge, 96°W-82° W, 7°N-17° N (Figure 2).

2.1. Geographic settings and geologic development

Guatemala Trench is formed in the place of the subduction of the Cocos Plate, which is is a young tectonic plate created as a results of the break of Farallon Plate into two tectonic plates: Nazca and Cocos. Cocos Plate is bounded by several tectonic plates: by North American Plate on the northeast, Caribbean Plate on the south, Pacific Plate on the west and by Nazca Plate on the south. Guatemala Trench marks the end of the North American continent up to the Guatemala Transverse Zone. Tectonically, the southern end of the North American continent is a special place, because of the changed direction of the plates compression: during the Late Cretaceous to the Paleocene, predominant type of compression was north-south between the North and South Americas, respectively, therefore the Caribbean thrust system was dominating. However, since Pliocene the dominant movement became a west-east strike slip (Aubouin et al 1982).

Cocos Ridge serves as a border for the wide continental margin of the Guatemala Trench. The Upper Jurassic-Cretaceous-Tertiary oceanic sediments occur in the slope of the Guatemala Trench, as well as in the Nicoya Complex of Costa Rica. Deformation across a convergent tectonic plate boundary of Guatemala Trench correlate with gravity-driven and subduction-driven tectonic processes. Guatemala Trench runs parallel to the ancient structures that can be explained by the processes of paleosubduction. On the contrary, the Acapulco Trench, intersects geologic structures of the southern Mexico. The differences in the south and northern parts of the Middle America Trench are notable on the land- and oceanward sides. Thus, the impact of the Tehuantepec and Cocos ridges differ on the seaward side, but very weak on the landward side of the Guatemala Trench. On the oceanward side, both ridges restrict Guatemala Trench from the continental shelf, but on the continental side, the Tehuantepec Ridge produces only a slight offset in the geological structures, whereas Cocos Ridge raises them as a whole (Aubouin et al 1982).

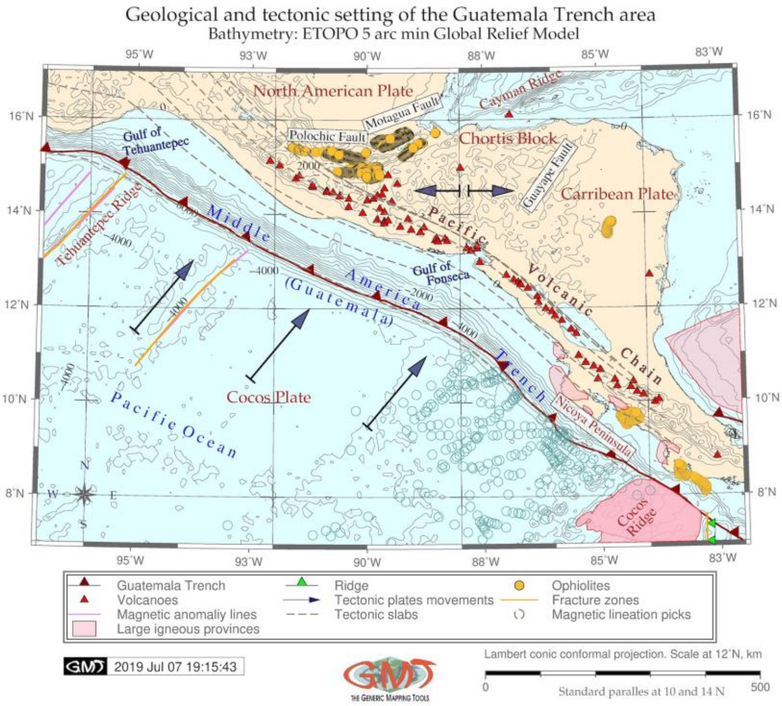

Figure 2. Geological settings of the Guatemala Trench

A system of major, active transform faults 'Motagua-Polochic system' consists of the Motagua Fault and Polochic Fault (Figure 2, north). The Motagua Fault runs across the Guatemala, continuing offshore until it merges with the Guatemala Trench near the Acapulco forming part of the tectonic boundary between the North American Plate and the Caribbean Plate. The Polochic fault lies north and continues Motagua Fault in parallel, sharing motion between the North American and Caribbean Plates (Lyon and Caen et al 2006). The Motagua Fault caused several major earthquakes, including the 7.5 Mw Guatemala 1976 earthquake. The geologic structure of the Guatemala Trench includes Paleozoic crystalline basement rocks, Mesozoic intrusive igneous rocks and sedimentary rocks spanning the Cretaceous to the Pleistocene.

The subduction of the Cocos Plate in the Palaeogene caused eruption of the volcanoes, which resulted in active melting and formation of magma. As a result, the Pacific Volcanic Chain is now notable along the Guatemala Trench (Figure 2). Some more notable geologic characteristics of the Guatemala Trench area visualized on the schematic map of the geological setting: bathymetry, tectonic plates movement directions, distribution of volcanoes, ophiolites, ridges and tectonic slabs. Northern part is marked by the Chortis Block (Figure 2), a group unit of rocks originated as a continental crust in Nicaragua. The Nicoya Peninsula (can be seen on the south-east on Figure 2) is formed by a volcanic-sedimentary series determined by radiolarian assemblages as Upper Jurassic and Cretaceous (Schmidt and Effing 1979). The distribution of the ophiolites is notable near the Polochic Fault and Motagua Fault (Figure 2), (Galli 1979).

2.2. Geochemical characteristics: rocks and minerals

Geochemistry of the sediments taken from the Guatemala Trench is presented by the olivine-plagioclase phyric basalts, the only presented igneous rocks is the study area, and plagioclase phyric high-alumina basalts. Basalts with thickness layer of 7 m covered by 150 m of sedimentary layers were detected on the Cocos Plate section of Guatemala Trench. The petrographic features of the trench basalts are typical for the basalts of the ocean floor: subaphyric, with plagioclase phenocrysts dominant over olivine phenocrysts, composed of abundant plagioclase microlites, olivine, clinopyroxene and rare spinel microcrysts, partly devitrified brown glass (Joron et al 1982). However, white some of the basalts are similar to the oceanic tholeiites, others have a composition transitional to island-arc tholeiitic basalts. As described (Dmitriev 1982), this indicate presence of magmatism in the zones of convergence of the oceanic, continental or island-arc crust.

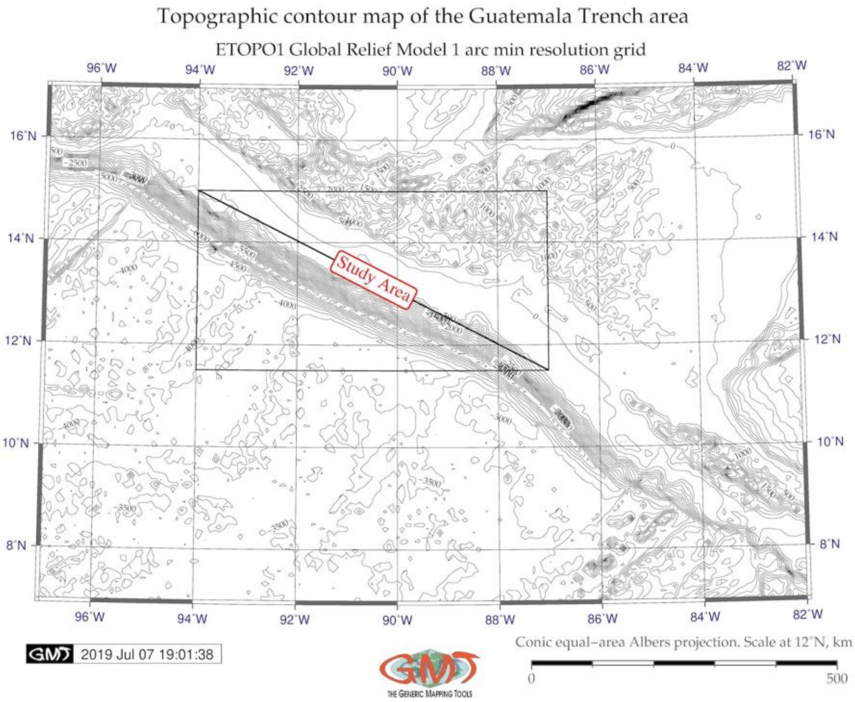

Figure 3. Topographic contour map of the study area: Guatemala Trench

Petrochemical setting of the basalts originated from the Guatemala Trench show compositions typical for the oceanic tholeiites and transitional to island-arc tholeiites with advanced differentiation of high-alumina varieties in both types of rocks. Namely, such transitional-type basalts differ from rocks of the oceanic and island-arc basalts by values of TiO_2 concentration and the $K_2O/K_2O/Na_2O$ ratio. Among other deep-sea trenches, chemically similar tholeiitic basalts are detected in the transects of the Philippine and Yap trenches. Furthermore, young age of some basalts from the oceanward slopes of the Guatemala Trench may indicate evidences of the local magmatism caused by the zone of convergence of oceanic and continental crust located nearby. This explains the eruption of the transitional basalts as oceanic and island-arc tholeiites in the Guatemala Trench. Secondary minerals of the basalts of Guatemala Trench in studied transects include smectite and chlorite, as well as talc, calcite, phillipsite, mica, and mixed-layer chlorite-montmorillonite also fill veins in the basalts of the trench (Kurnosov and Shevchenko 1982).

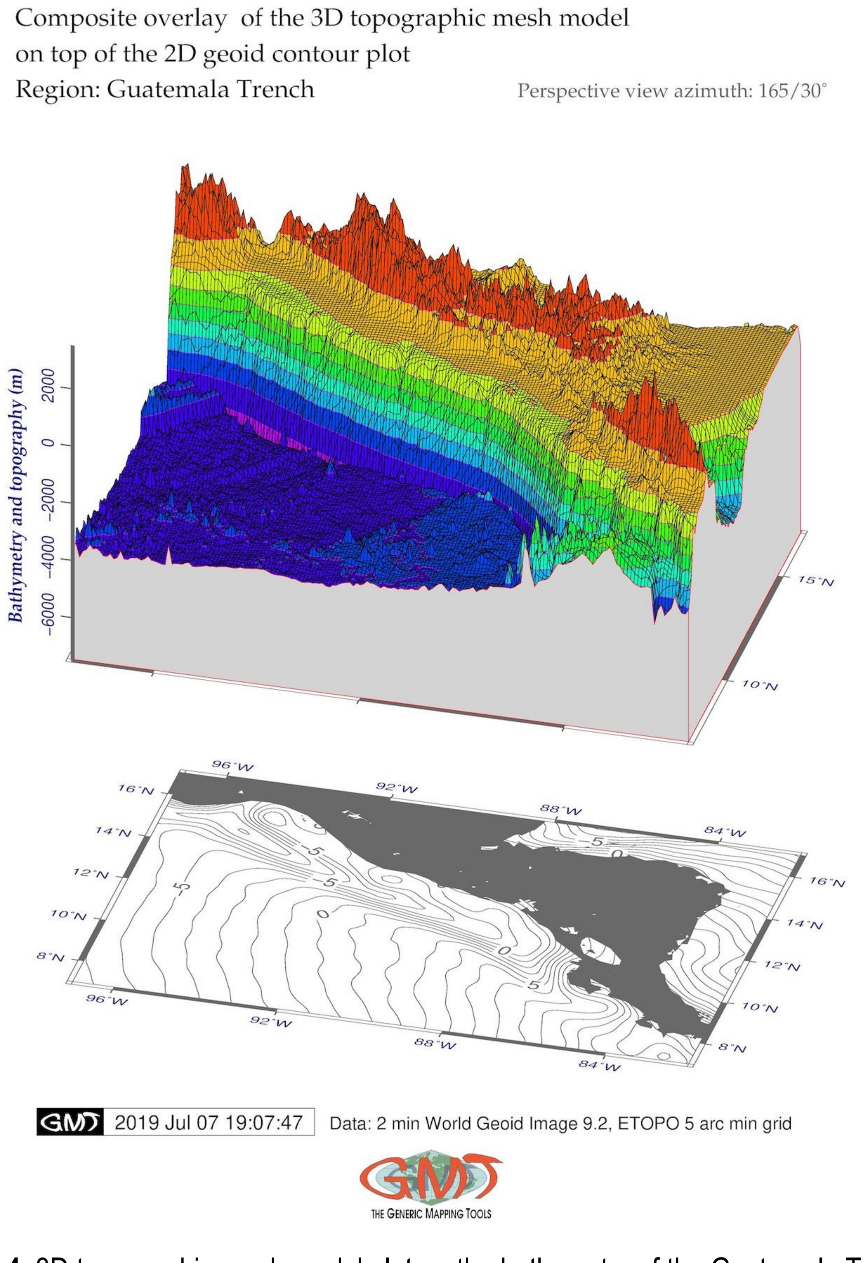

Figure 4. 3D topographic mesh model plot on the bathymetry of the Guatemala Trench

Marine biological analysis of the samples taken from the Guatemala Trench (Shipboard Scientific Party, 1982a) shows calcareous benthic, planktonic foraminifers, and calcareous nannoplankton recovered within the sediment cores along the trench axis that show relatively high faunal diversity. Their presence at great depth indicates rapid sediment transport and burial. The abundance of the biogenic silica throughout the sediment section indicated that continental slope of Guatemala Trench had high biological productivity environment. The conglomerates of the trench indicate rapid sedimentation of the deposits accumulated in a trench slope that proved a relatively quiet environment of sediment deposition (Coulbourn 1982).

Samples from the Guatemala Trench revealed areas composed of the hemipelagic muds containing substantial biogenic components that proves a high degree of bioturbation: samples consist of diatoms, radiolarians, sponge spicules, calcareous nannoplankton and foraminifers of lower to middle bathyal benthic species (Shipboard Scientific Party, 1982b). The 'Glomar Challenger' expedition sampling shown that selected spots on Guatemala Trench predominantly consist of dark olive gray biogenic muds.

The terrigenous component of the sediments is dominant and consists of clay minerals and minor contributions of the volcanic glass. The biogenous contribution is secondary and consists of ca. 50% diatoms and nannofossils as well as biogenic debris (foraminifers and sponge spicules).

2.3. Geomorphology and sedimentation

Brief sedimentation history of the Guatemala Trench area was well summarized by Kurnosov et al (1982): the sedimentation on the continental slope was supplied by a smectite- and plagioclase-rich terrigenous land source area during the Late Cretaceous. A volcanic source existed in Guatemala Trench area in middle Miocene, as proved by the volcanic glasses followed by the persisted volcaniclastic constituents. Major sediment types of the Guatemala Trench include turbidites, hemipelagic sediments, chalk, basalt and slope sediments (Ross 1971).

The sedimentation processes on the trench began in early Miocene with increased accumulation of the metalliferous foraminifer-nannofossil ooze above the basalt basement. The basal chalk, a source of Fe and Mn, presents a typical mid-oceanic metalliferous sediment type, located near the spreading center of the Guatemala Trench. A sedimentation time gap at Guatemala Trench in the middle Miocene to early Pliocene refers to a radiolarian-bearing pelagic clay and weak supply of terrigenous sediment at this period. In turn, it may indicate on the remote location of the site from the land masses. The Cocos Plate moved away from its spreading center toward the subduction zone in the Guatemala Trench during this period.

During Pleistocene period, the hemipelagic sedimentation was substituted for the turbidite accumulation that reached present location on the seafloor of the trench. Sites located at the juncture of the Guatemala slope and the trench seafloor contain biogenic debris, including wood fragments. The sequence of the Quaternary trench-filling turbidites is either faulted or deposited against a fault scarp in lower Miocene chalk on the detected sites of the trench (Shipboard 1982c, Cowan 1982).

Lithologic variation and different compaction states at the trench show (Faas 1982) that sediments on the continental slope have identical compaction as sediments in the trench, yet their compaction curve is intermediate between pelagic clays and diatom ooze. The sediments in the Guatemala Trench have intermediate compaction level between pelagic clays and terrigenous sediments which is caused by the mixing of pelagic sediments with the terrestrially derived turbidites. Another particular feature of the trench consists in partly consolidated lower Miocene to Quaternary hemipelagic muds that contain vertical-subvertical veins, < 2 mm thick, spaced from one to several millimeters apart. Apart from the Guatemala Trench, such morphologically analogous structures were obtained from the inner slope of the Japan Trench.

The ocean crust of the Cocos Plate subducting beneath the landward slope of the Guatemala Trench has a linear horst and graben topography of 100 m relief. This passive assimilation of the oceanic material occurs without disturbing topography shape. The subduction of the horst and graben topography in the Guatemala Trench area is largely passive and locally active. The mid-slope area has a rugged topography covered by thick slope deposits while lower slope is relatively smooth except local brakes by benches. Upper and middle slope areas correlate with strong magnetic anomalies. Rough midslope topography may reflect erosion following the Paleocene uplift and local subsidence in early Miocene. Slope deposits covered landward slope of the trench, which correlates with the increased arc volcanism indicated by ash layers (Huene et al 1982). A thick sequence of the terrigenous sediments was discovered seaward of the Middle America Trench (Shipboard Scientific Party 1982d).

More detailed insight to the origins of the geomorphology of the Middle America Trench in its both parts, Acapulco Trench and Guatemala Trench, and factors affecting landform formation, were extensively studied in relevant papers (Shipboard Scientific Party 1982e, Alvarez Gomez et al 2008, Shipboard 1982499, Azema and Tournon 1982, Alvarez Gomez et al 2012).

3 METHODS

3.1 Research Emphasis

The aim of this research was to develop a method for spatial modelling of the Guatemala Trench geomorphology, analysis of its bathymetric characteristics (depth, slope steepness), geomorphic shape of its submarine landforms and surface trends in topography and gravity grids that reveal unevenness in its structure. The methodology goal was to find geometric particularities of the trench in its western and eastern flanks to represent correlation of the submarine geomorphology characteristics with geologic settings and seismicity of the Guatemala coasts. Modelling cross-section profiles was aimed to detect major depth observation samples at different parts of the transects and seafloor segments. The methodology is based on detailed geospatial database containing raster grids on bathymetry, gravity, geoid and geological vector layers.

Research gap consists in the lack of detailed studies specifically on geomorphic characteristics of the Guatemala Trench, caused by its unaccessible location. The remote located of the deep-sea trenches often means that trench slope and steepness, width and curvature is ignored in geomorphological descriptions, which may increase uncertainty in our understanding of their form and possible connections with underlying geological settings. However, geometric properties of the trenches, such as slope steepness, width and depths across their various segments vary and may be set to variables for consideration in further spatial models. Alternatively, trench morphology may be estimated by empirical functions of stability, seismicity and similar geological numerical models.

Research goal is to determine to what extent the results of the geomorphological assessment of the trench correspond with the geological settings along its various segments from Tehuantepec Ridge to Gulf of Fonseca. Potential correlation of bathymetry with geology along the trench profiles can be caused by the closeness of the Pacific Volcanic Chain with notable seismicity, increasing sedimentation intake to the trench over considerable distances. Modelling geometric profiles of the individual segments of the trench was aimed to be a supplement to the general geomorphological analysis of the trench performed as a GMT based comprehensive geospatial assessment.

Additional goal was the creation of several thematic maps of the region (geology, gravity, geoid) capturing patterns in the seafloor geophysical settings utilizing datasets collected through data mining. Visualized geophysical and geological features include tectonic slabs lineaments, ophiolites, geoid and gravity values, fracture zones and selected seafloor features, such as seamounts. Certain similarities between this geologic settings, geoid and marine free-air gravity models can be seen (e.g. correspondence between some of the geology lineaments and isolines, particularly in Figure 5, Figure 6 and Figure 2, and the trench main axis.

The objective of this research was to model geomorphological profiles of the Guatemala Trench, digitized at 400 km long segments, spaced between 20 km and sampled every 2 km, using a sequence of GMT modules with main ones 'grdtrack' and 'trend1d'. In addition, this work is intended to establish a framework of the geospatial modelling and mapping using multi-source data to obtain a better understanding of the submarine shape of the trench, and to raise awareness of this unique location. Hence, this investigation is the first of its kind focused on the Guatemala Trench, a southern part of the Middle America Trench, to provide quantitative measurements of its geomorphological and topographic impacts caused by the geological settings, tectonic historical development and high seismicity in the region, being the most important mentioned factors. This paper contributes towards investigation of the geomorphological modelling of the deep-sea trench as a part of the complex seafloor geomorphic system in the context of tectonic interaction between the Cocos, Pacific and Caribbean tectonic plates.

3.2 Data and Tools

Dataset used in this study was acquired through the data mining undertaken to search for publicly available bathymetry data which included following datasets:

1. Global Relief Model ETOPO1and ETOPO5 (Amante and Eakins 2009), DEM from NOAA
2. EGM96 (Sandwell et al 1995; Sandwell et al 2013)
3. Vector Global Self-consistent Hierarchical High-resolution Geography Database dataset embedded in GMT (Wessel and Smith 1996).
4. Gazettier of International Hydrographic Organization (IHOIOC 2012).
5. Global Volcanism Program (GVP) database compiled by Smithsonian Institution, U. S.
6. Geologic datasets (tectonic plates boundaries, slabs, lineaments, trench lines, ophiolites, volcanoes, etc) from Scripps Institution of Oceanography (SIO).

The main tool for the presented research is Generic Mapping Tools (GMT), a cartographic scripting toolset developed by Wessel in Smith (Wessel and Smith 1995). Comparing to the traditional GIS software used and tested in geospatial research with the most often as ArcGIS (Suetova et al 2005a; Lemenkova 2011; Klaučo et al 2017; Kuhn et al 2006; Lemenkova et al 2012; Klaučo et al 2013; Suetova et al 2005b), the advantages of the GMT consists in flexibility through scripting approaches rather than GUI, as well as open source availability. Besides, a great advantage is a cartographic functionality of the tool set: a large variety of the visualization, plotting, modelling, as well as advanced cartographic modules (projections, modelling, grid data processing).

3.3 Topographic and geological mapping

General bathymetric map (Figure 1) was mapped using original ETOPO1 raster grid with 1 minute (Amante and Eakins 2009) resolution. The map was visualized on the study area square using a sequence of the GMT modules. A 'grdcut' module was used for cutting area of interest from the global grid earth_relief_01m.grd by selecting coordinates -R263/278/7/17, following by 'grdimage' module for visualizing the grid itself. Several auxiliary modules were then used both for cartographic purposes (color scale, scale bar, directional rose, grid ticks and lines, etc) and for the map embellishment (GMT logo) using available techniques. The shoreline vector layers were driven from the existing GMT data sets (Wessel and Smith 1996): tectonics, bathymetry, geomorphology and geology. The bathymetric data are presented as plan and oblique shaded-relief grids to highlight the major and distinct seafloor landforms of the trench (Figure 1) mapped using the GMT scripts.

Topographic data were collected rom the ETOPO5 from 5 arc min covering seafloor bottom bathymetry as well as coastal topography covering study area. The modelling was performed using GMT module 'grdview' followed by a sequence of auxiliary GMT modules (grdcut, grd2cpt, grdcontour, pscoast, grdview, logo, psconvert). Additionally, some UNIX progs (rm, echo) were used. The initial data was cut off from the 5 minute grid using GMT 'grdcut' module: gmt grdcut earth_relief_05m.grd -R263/278/7/17 -Gmat_relief.nc.

The ETOPO dataset includes a variety of the resolution that can be selected for the data source. ETOPO5 was selected as a base grid for 3D mesh plotting, to avoid small-scale irregularities which tend to visually overload the derived topographic attributes, making 3D mesh overlay visually complex. For the case of 3D-mesh grid model (Figure 4), the purpose was to create a visualization overlay that highlights the geomorphic surface of the trench and adjusting continental steep slope. This allowed a smoother visualization of the 3D-mesh polygons by removing some of the finer detail in 3D mesh plotting. Afterwards, the rotation azimuth was set as -p165/30° with an overlay distance from the geoid contour at 4,5 cm.

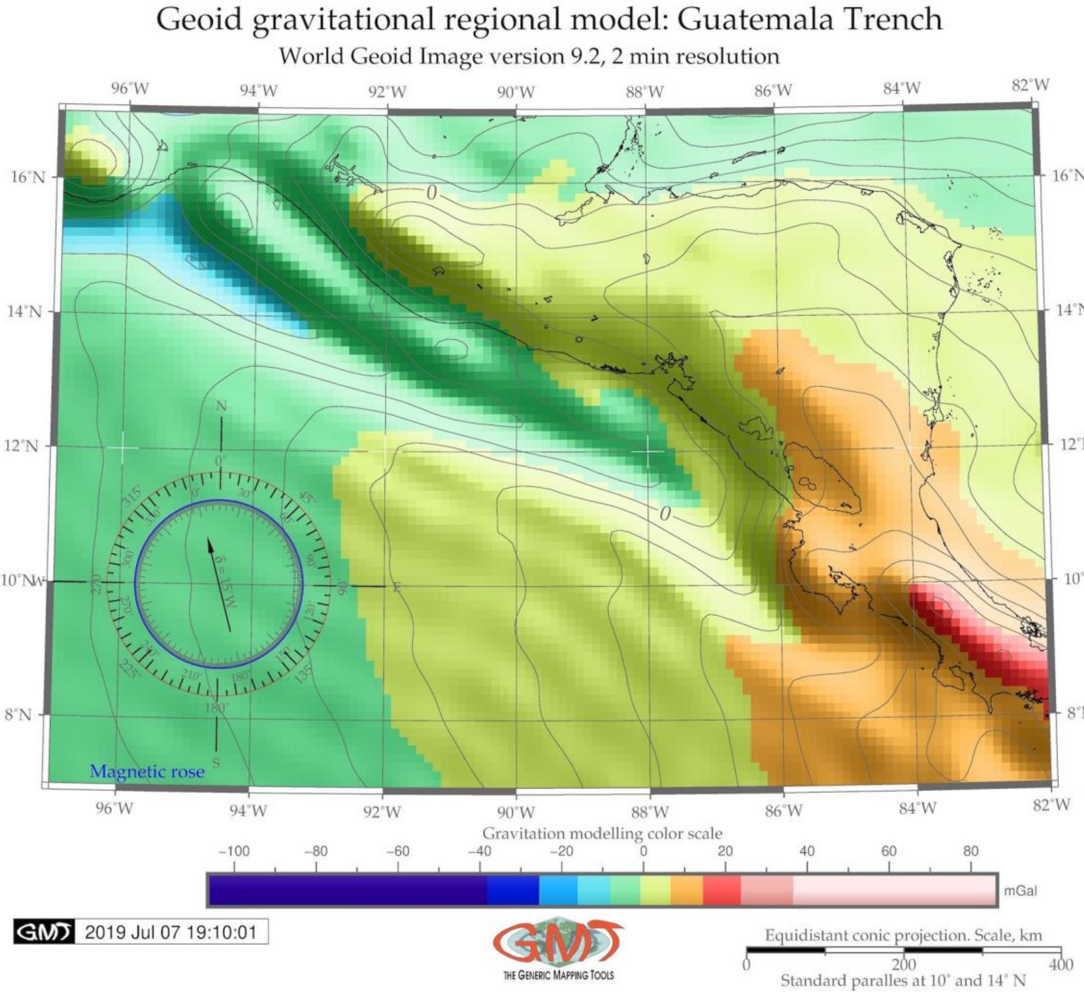

Figure 5. Geoid model of the Guatemala Trench

The background geoid contour (a 2D plane grayscale map below the map, Figure 4) was plotted using GMT module 'grdcontour' by the following command: gmt grdcontour geoid.egm96.grd -JM3.5i -R263/278/7/17 -p165/30 -C1 -A5 -Gd3c -Wthinnest,dimgray -Y3c -U/-0.5c/-1c/" Data: 2 min World Geoid Image 9.2, ETOPO 5 arc min grid" -P -K >ps' Here the contour lines are given by every one with annotations at every five (-C1 -A5). The rotation of the 3D grid was chosen at the angle most corresponding to the visualization of the trench, after several trials at different angles, depending on the oblique rotation and depth. A plane was drawn at -7500 m s z-level with dimgray color provided via the +g modifier to highlight the frontal facade between the 3D plane and the data perimeter and -Wf0.1p,red setting used for the pen outline. The output 3D model is presented at (Figure 4).

3.4 Geophysical modelling of geoid and gravity

Geophysical concept of the geoid and gravity model consists in the following aspects. Earth's interior has distinct variations in density which causes geoid undulations and anomalies of gravity models. The geoid model highlights oceanographic properties of the study area: a mathematical shape of the ocean surface with the only impact of the gravity and rotation, without other impact factors (e.g. winds and tides).

In turn, the structure and submarine geomorphology of the ocean trench is affected by Earth's interior through tectonic plates subduction and movements. therefore, visual shape of the geoid and gravity is distinctly repeating the bathymetric isolines (Figure 1, Figure 5 and Figure 6). Thus, a modeled geoid presents a smooth yet irregular surface with visualized shape resulted from the uneven distribution of the mass on the Earth's surface. Modelling geoid (Figure 5 for the study area was performed using a sequence of the GMT modules: gmtset, grd2cpt, grdimage, pscoast, grdcontour, psbasemap, psscale, psimage, logo, pstext, psconvert. Technical workflow for the generated model is as follows. A color palette table was generated from the grid by the following GMT command: gmt grd2cpt geoid.egm96.grd -Chaxby > geoid.cpt. Afterwards, the geoid image with shading was generated by the following GMT code: gmt grdimage geoid.egm96.grd -I+a45+nt1 -R263/278/7/17 -JD270/12/10/14/6i -Cgeoid.cpt -P -K >ps. Additional cartographic elements were added using GMT basemap module: grid, title, costline and GMT pscoast module. The geoid contour was generated by the following command: gmt grdcontour geoid.egm96.grd -R -J -C2 -A5 -Wthinnest,dimgray -O -K >>ps

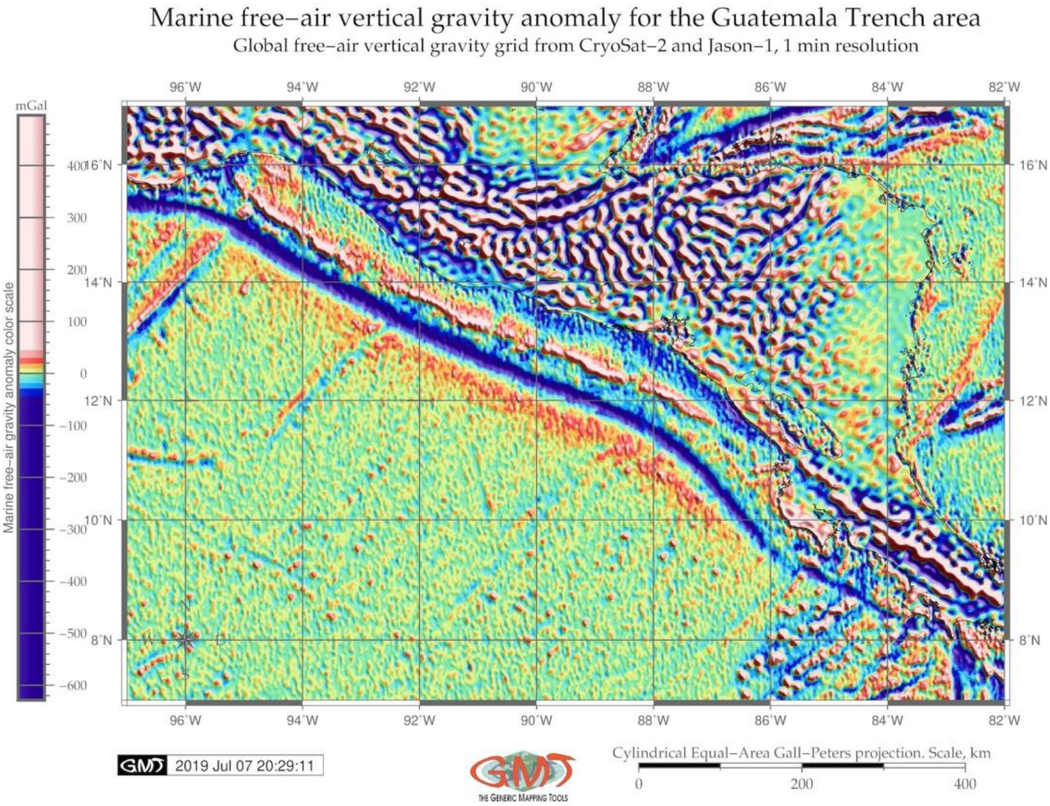

Figure 6. Gravity model of the Guatemala Trench

Marine free-air gravity and vertical gravity anomalies (Figures 6 and 7) were modeled using original grid base on the CryoSat-2 and Jason-1 source data with 1 minute resolution, described in relevant publications (Sandwell et al 2014, Sandwell et al 1995, Sandwell et al 2013, Smith and Sandwell 1997b). Key GMT code to generate the gravity mode was based on 'grdimage' module that generated gravity image with shading: gmt grdimage gravMAT.grd -I+a45+nt1 -R263/278/7/17 -JY270/12/6.5i -CgravMAT.cpt -P -K >ps. Here the -R function shows selected region (263$°-278°W, 7°-17° N, the JY270/12/6.5i stands for cylindrical equal-area Gall-Peters projection and 6,5 inches the overall dimensions of the map; -I+a45+nt1 shows the illumination and -CgravMAT.cpt selects the color palette created on the previous step. Chosen color palette (GMT_haxby) shows transition from lower gravity values (<20 mGal) to higher (>90 mGal).

The dataset of this research was augmented by free ASCII data on gravity and topography as xyz table, collected from the available source in a table format from USGS: http://topex.ucsd.edu/cgi-bin/get_data.cgi The data range was set to the following coordinates square (here with a systems of 0-360; 0-90 rotation): Lon 263°/278°; Lat 7°/17°. According to the gravity data inspection (gmt info grav_MAT.xyz), the range for the data is as follows: total number of points = 554115; minimal value is -157.1 mGal at point with coordinates 263.0083° 7.0076°; maximal value is 452.4 mGal at coordinate 278.0083° W/ 17.0032° N. Based on this, the color palette was adjusted accordingly to the data range: gmt makecpt -Ccyclic.cpt -V -T-160/455 >

surface.cpt where -T-160/455 shows the min/max data. Thereafter, before modelling surface, the data were interpolated for the correction for the source data by generated 1 by 1 minute block for the mean values from the raw ASCII xyg table. Afterwards the data were processed using 'gmt surface grav_MAT_BM.xyg -R263/278/7/17 -T0.25 -I30s -GSurface_MAT.nc -Vv' command, which modeled the surface from the xyz data.

Both topographic surface modelling (Figure 8) and gravity surface mapping (Figure 9) are based on the modelling numerical ASCII data in xyz format to the netCDF format (Rew and Davis 1990). The gradient illumination was added to intensify the surface with azimuth 45° using gmt grdgradient module with shading azimuth gradient 45°. Added illumination on the shaded image highlighted topographic pits, furrows and submarine landforms on the seafloor of the Guatemala Trench. The data were color coded by the cyclic color palette (cyclic.cpt) with the resulting image shown in Figure 9. The raster image output was created using GMT command 'gmt grdimage Surface_MAT.nc -Csurface.cpt -R263/278/7/17 -JM6i -P -ISurface_MAT.int -Xc -K > ps'.

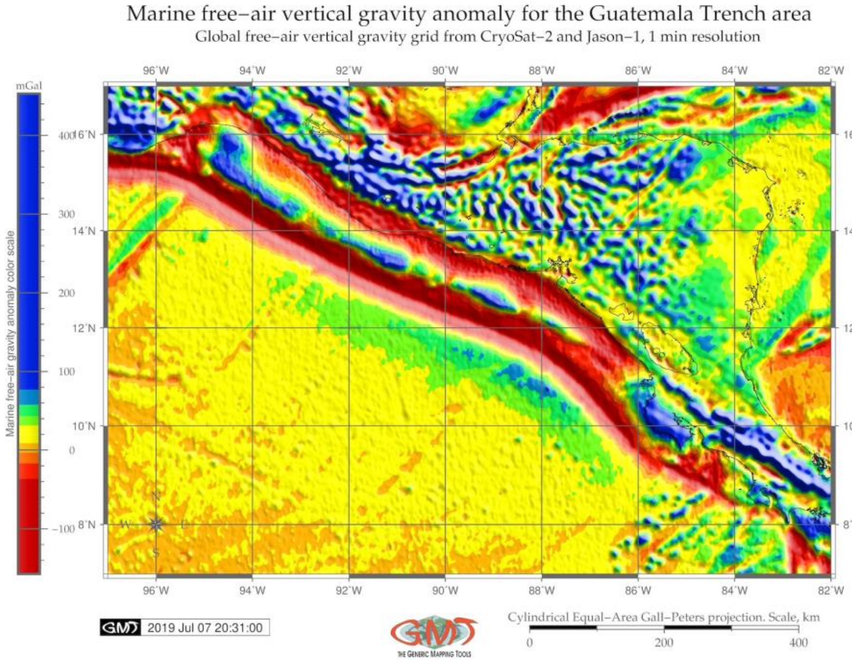

Figure 7. Vertical gravity model of the Middle America Trench.

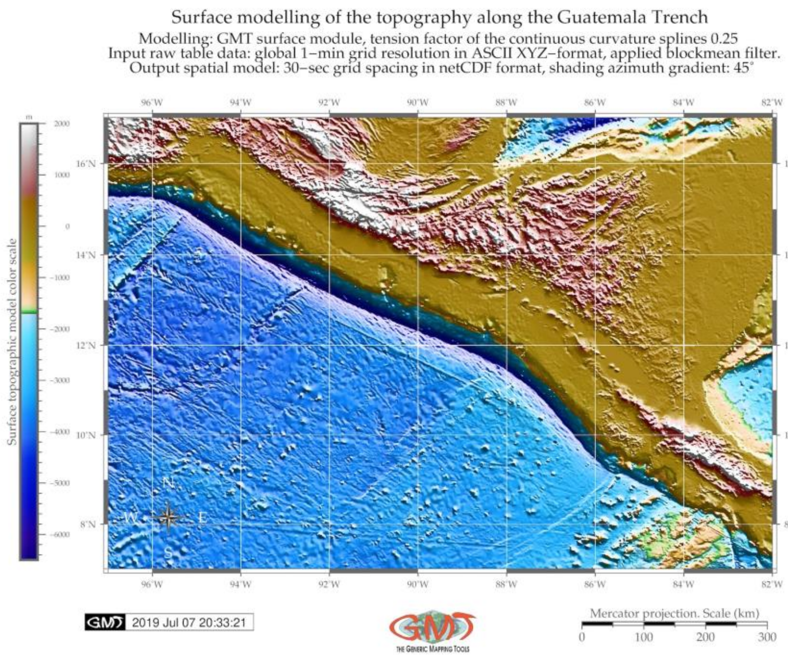

Figure 8. Surface modelling: topographic map generated from the ASCII xyz data

Additional cartographic elements (ticks, legend, scale bar, grid lines, directional rose, etc) were plotted using GMT modules. For instance, drawing grid was performed using command 'gmt psbasemap -R -J -Bpxg6f2a2 -Bpyg6f1a2 -Bsxg2 -Bsyg2 -B+t"Surface modelling of the gravity along the Guatemala Trench" -O -K >>ps. The 1 m bathymetry and xyz grids were interpolated to 30-sec m resolution and a grid derived from the bathymetry and gravity were visualized. Depth, and gravity contours in mGal were derived with tension factor of the curvature splines at 0,25, respectively. Modeled data were then exported as a 30-sec resolution grid spacing in netCDF grid.

Minor study area is bordered by the square with coordinates: 94°W-87°W, 11,5°N-15° N (Figure 3). In total, a data set of the 21 underwater cross-section transects were digitized automatically along the selected segment of the Guatemala Trench within the study area. Technically, the main GMT module 'grdtrack' was accomplished by a sequence of the auxiliary modules. The full details of the GMT bash code sequences and characterization of the module options and elements in comments including UNIX progs (echo, rm, cat). The orthogonal cross-section bathymetric profiles were drawn automatically using presented script across the Middle America Trench with a length of 400 km (Figure 10).

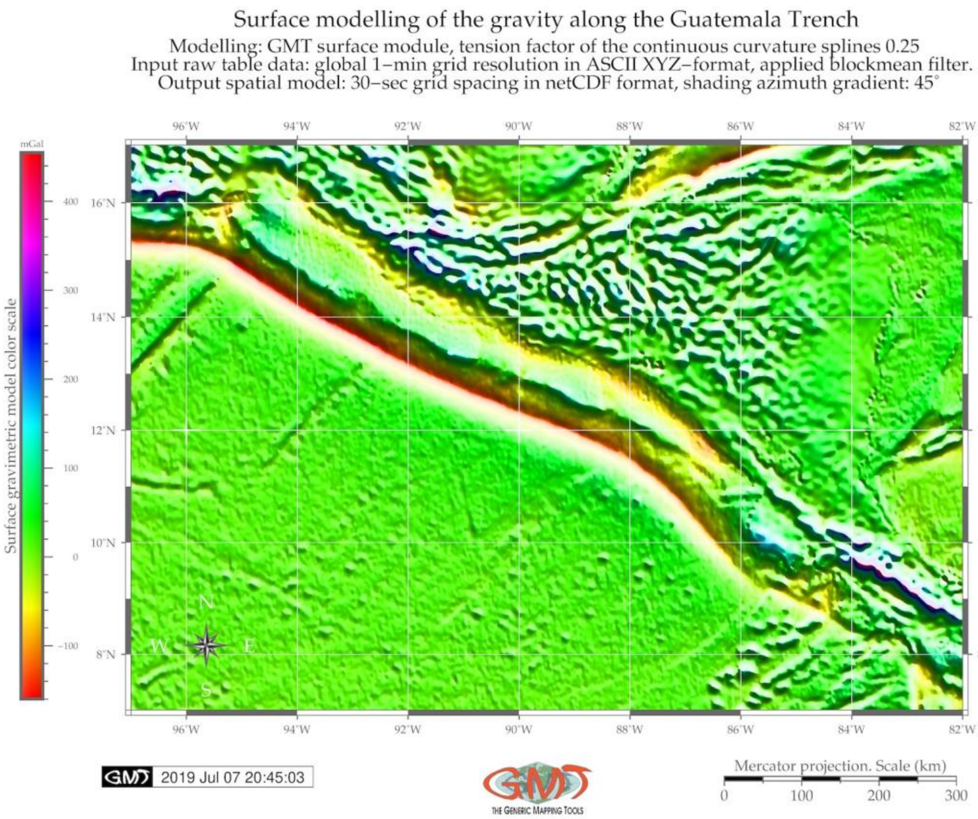

Figure 9. Surface modelling: gravity model generated from the ASCII xyz data

3.5 Automatic digitizing of the cross-section profiles

Plotting cross-sectional profiles, or transects, along the selected segment of the study area is a common technique in geological investigations. Examples of the geological cross-section profiles plotting, automatic digitizing and marine data analysis can be seen (Ross and Shor 1965, Moore et al 1982, Lemenkova 2019a, Schenke and Lemenkova 2008; Lemenkova 2018b). Cross-section orthogonal profiles were taken through key seafloor features at the coordinates 268.4°W 13.0°N 271.9°W 11.6°N to show the variety of the steepness angles. Cross-track profiles are 400 km long, spaced 20 km, sampled 2 km to achieve sampling evenness. Depths values were calculated by each profile, and their mean and median values were modeled thereafter. The output model is showing the initial bathymetric map (Figure 10 B) and a plotted series of the profiles above (Figure 10 A).

However, terraces were less well defined, perhaps due to the local specific geomorphic features of the study object: the geomorphology of the trench presents a very straight steep slopes without significant curvatures. Automated digitizing process increased precision and speed of plotting, and highlighted submarine geomorphic features, such as oceanward backers of the trench and more steeper slope on the continental side.

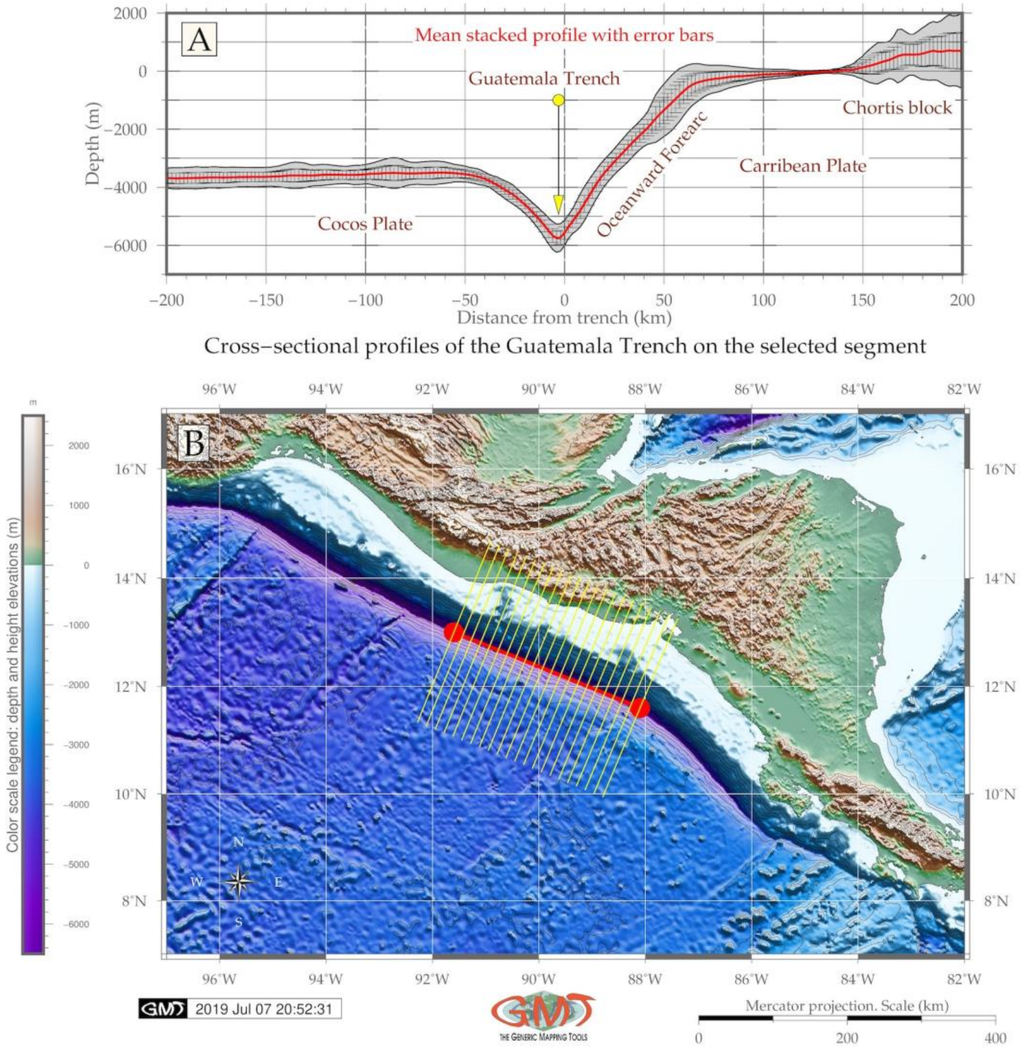

Figure 10. Cross-section profiles on the selected segment of the Guatemala Trench

3.6 Statistical analysis

Statistical data processing was performed using table generated through digitizing profiles at the previous working step. The description statistical analysis include modeled trend regression for the cross-section profiles (Figure 11), computed trends for the profiles curves and plotted two types of the statistical histograms: a rose diagram and a standard box histogram (Figure 12). Modelling was done to visualize mathematical approximation of the curvature of the geomorphological profiles, which fits a weighted, robust, polynomial, and Fourier model for the formula y = f(x) to xy(w) data. Four types of approximation models are made by 'trend1d' GMT module and presented to analyze the curvature of the profiles. The resulting graph of the trend regression models for the cross-section profiles of Guatemala Trench was plotted using GMT script: Figure 11.

The explanations of the plotted curves is as follows. The first graph (Figure 11, E) shows a basic LS line based on the formula $y = a + bx$ and done using code gmt trend1d -Fxm stackMAT.txt -Np1 > modelMAT.txt. It shows Fourier series with t terms where the '-F' stands for Fourier approximation in the code. The second graph (Figure 11, D) shows approximation of the curve according to the formula $y = a + bx + cx^2$ representing single Fourier component of order n. It was plotted using code: gmt trend1d -Fxm stackMAT.txt -Np2 > modelMAT.txt. The third graph (Figure 11, C) has been computed by formula $y = a + bx + cx^2$ using code gmt trend1d -Fxmr stackMAT.txt -Np2,f1+l1 > modelMAT.txt where the '+r' component is added as an appendix in the code +r for a robust solution. Finally, the fifth graph (Figure 11, B) shows plotted residuals of the graph with respect to outliers. Discussions on mathematical approximations are presented (Menke 1989).

Statistical histograms of data distribution were plotted using a sequence of the GMT modules: gmtset, psrose, pshistogram, pslegend, logo and psconvert. The histograms plots demonstrated frequency of the data distribution against bathymetric variables. The statistical techniques of the data analysis are widely used in geospatial studies, applied and described in previous works (e.g., Marques de Sa 2007; Lemenkova 2019c; Lemenkova 2018b, Lemenkova 2018a). Current study applied histogram techniques showing depths distribution along the profiles. Unlike traditional statistical data analysis that utilizes standard tools for this purpose, such as R and Python libraries, Gretl, SPSS, MATLAB/Octave (Lemenkova 2019b; 2019d; 2019e; 2019f), this research shown statistical visualization by GMT using modules 'pshistogram' and 'psrose'.

4 RESULTS

Multiple factors affect Guatemala Trench geomorphology which include among others mechanisms of the tectonic plates subduction, lithology, sedimentation processes, closeness of the volcanic active zone, geochemical content of the substrate and other geological factors.

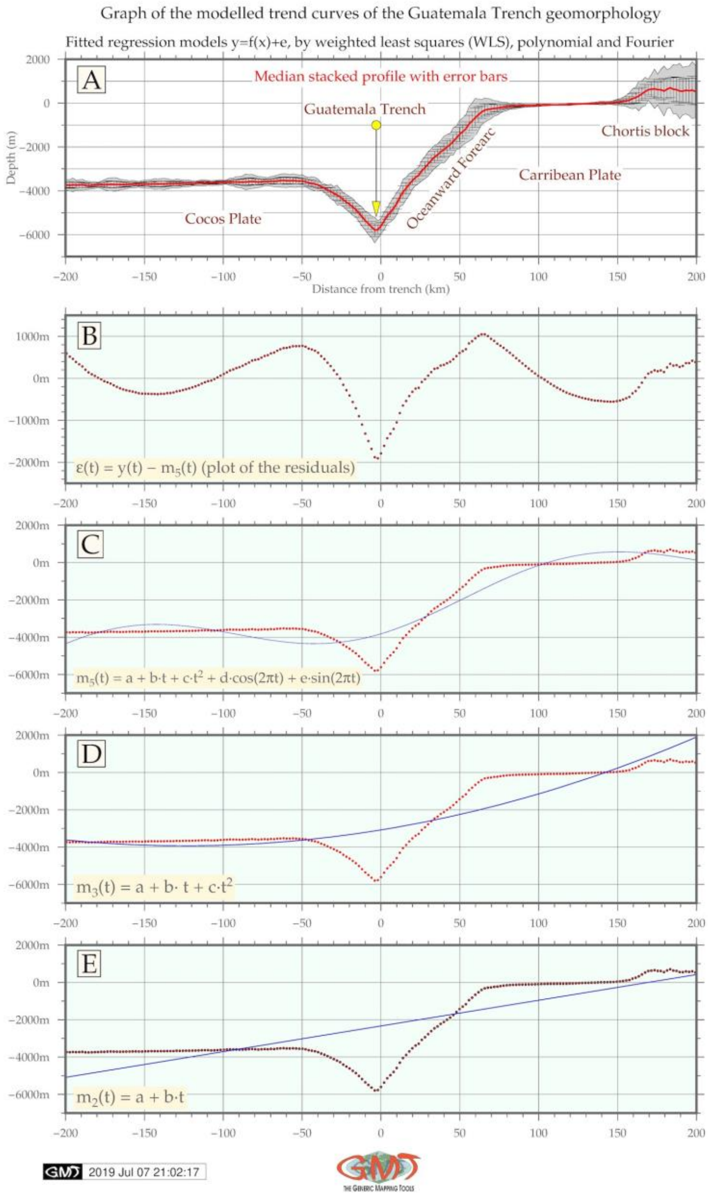

Figure 11. Trend regression models for the cross-section profiles, Guatemala Trench

The trench is formed as a result of the complex interaction between these factors. Generally, a strong correlation of the trench's axes with borders of the two tectonics plates (Pacific Plate and Cocos Plate) is evident. This implies that the geomorphology of the trenches is strongly correlated with slabs, since continuation of the plate movements, lineaments and extend of fracture zones leads to the formation of the trench axis strongly determined by plates motions. The geological local settings, stretch of the tectonic slabs, complex tectonic processes and sedimentation of the Vanuatu and Vityaz trenches explain differences in their structure and geomorphic shape form. Cartographic mapping and data in 2D reveal physical shape, structures and visualization of the objects, but 3D dimensional visualization is a useful addition for a visual analysis of the geomorphic shape of the objects. In view of this, local 3D model atop of the planar mode of the ETOPO1 were plotted to visualize the form and comparative view of the trenches (Figure 7).

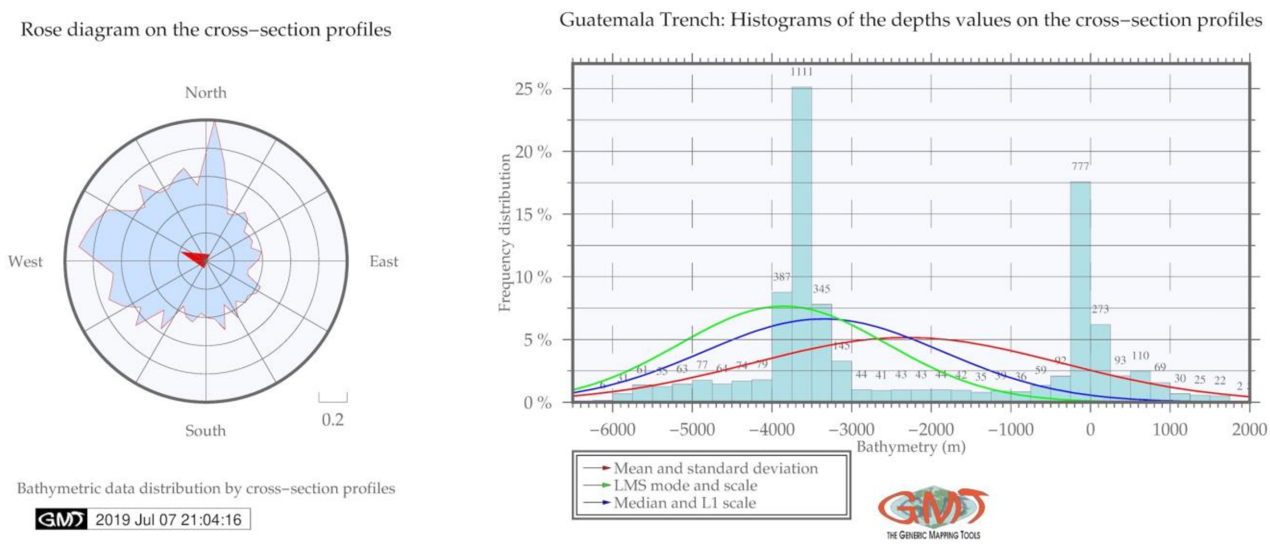

Figure 12. Histograms of the sample data distribution by the cross-section profiles

Modelling geospatial data highlighted geomorphic shape and geometric properties of the trench. The geometry of the trench demonstrates its relatively steep and strait shape which correlate with previous seismic record results (Shipboard Scientific Party 1982d) showing trench floor 3-5 km wide. Spatial analysis revealed that major depth observation points of the trench are located in between the -3000 and -6200 meters (Figure 10 and Figure 11). The position of the bathymetric observations in trend analysis (Figure 11, A) indicates general trend similarities in the seafloor characteristics between the geomorphic units. Figure 11, A shows clear division between the oceanward slope with steeper angle Cocos Plate basin, trench valley and rocky Charts block unit.

The geometric form of the trench has a symmetric accurate 'V' shape for the segment of -30 to -30 km on the graph (Figure 10, A). On the oceanward side (right on the graph) further slope increases towards the continental shelf, while left flank stabilizes in depths at the distance of -50 km from the main axis. Here, the depth to the bottom of the trench becomes gradually deeper in a segment of -50 to 0 m in a cross-section, decreasing from -3,200 to -5,800 (median red colored line on the graph). The right (oceanward) side of the trench is dipping eastwards with 35,63° slope at the distance 0-20 km from the major axis. The next segment (20-40 km) has a steepness of 42,17° from the vertical plumb line, and 44° at the segment of 40-60. The left side of the trench has 43,24° at the distance of 0 to 24 km from the main axis, which then decreases to 28,33° at 24-40 km, followed by a segment of 14° at the segment of 40-60 km off the trench axis. The last and longest segment of the graph (a distance from 60 to 200 km on the left flank of the graph (Figure 10, A) has almost no changes in slight elevation decrease with only 1,13° westwards.

Frequency data distribution of the observation samples shown notable changes within the Guatemala Trench by the profiles. There is a certain increase of frequency in depths between -3000 and -4000 m (Figure 12) that might be caused by the specific geologic properties of the Cocos Plate.

The deepest depth data range with 1,111 records takes 25% of the total pool of the sample observation points. As can be seen on Figure 12, right, means of the observation samples have a value of -2,200, while LMS mode indicates 7,5% of values at -4,000 to -3,500 m, and medians have values of -3,200 to -3,300 m. A North-West distribution of the rose diagram (Figure 12, left) shows steep slope on the oceanward forearc of the trench with relatively few observation samples due to the steepness on the continental slope with denser samples on the Cocos Plate where the geomorphology has more gentle form that can also be noted on (Figure 10, A).

A geoid gravitation model differs significantly by movements in a south-east direction along the study area with clearly detected stripe of the Pacific Volcanic Chain (Figure 4). Maximal values of the gravity > 20 mGal are recorded in the south-eastern part of the region Nicaragua: Nicoya Peninsula and Costa-Rica (colored red on the modeled map). The area of Nicaragua mostly has values of 5-15 mGal (colored orange on the modeled map). The area of Gulf of Tehuantepec has the lowest detected gravity values in the range of -15 to -25 mGal (Figure 4). Marine vertical gravity at the trench demonstrates correlation of contours of the major lines with tectonic slabs. The intermediate values (20-30 mGal) are located on the trench slopes (colored orange on the Figure 6), while the highest values are detected mainly on the mountainous areas (colored rose on the Figure 6). This suggest that submarine geomorphic structure of the Guatemala Trench has a straight shape form of the slopes with more steep slope on the oceanward forearc.

Free-air gravity map (Figure 6) was plotted using conceptual approach of the marine gravity field modelling, described by Smith and Sandwell (1995). It illustrates values (mGal) of the density anomalies at bathymetry, sediments, crust and mantle in the region of the trenches. The free-air anomaly is dominated by the short wavelength variations which reflect the density contrast at the seafloor. Accuracy of the marine gravity measurements is important for the data modelling (Wessel and Watts 1988). Therefore, modelling free-air gravity model was done based on the data from high quality raster grids showing gravity anomaly model from the Scripps Institute of Oceanography: CryoSat-2 and Jason-1 Sandwell et al 2014.

5 DISCUSSION

A phenomenon of the tectonic plates subduction is being reflected by the geometric asymmetry of the deep-sea trench, which is formed in the empty space between one plate subducting down to the mantle and another being deformed. Bathymetry of the trench is influenced by other geophysical and geological processes and factors affecting its shape and structure. However, correlation between the geomorphology and underlying physiographic settings of the seafloor confirms that tectonic plates and slab geometry are the main factors controlling its form, slope gradient steepness and depths. Geomorphology and shape of the oceanic trenches are profoundly inaccessible. Great depths and remote location of the trenches explain that mapping submarine areas is a laborious process that requires advanced methods of data analysis. Currently, seafloor mapping remains the most difficult task in modern cartography.

Visualization is a central concept in geoinformatics. Cartographic functionality of GMT provides a variety of modules for effective and accurate mapping which enables not only visualization of the raster and vector layers, modelling graphs and performing statistical analysis, but also aesthetics, fine tuning of the graphical output, legends, layouts, color palettes, selection of projections, variety of fonts and visualization approaches and other tools of the cartographic design. The actuality of the presented research is explained by the advantages associated with geologic exploration of the seafloor, and appreciation of the form of the oceanic landscapes.

However, due to its specific scripting approach of GMT, there is not enough existing experience of the detailed workflow based on the GMT mapping, comparing to the traditional GIS. Existing papers based on GMT (e.g. Ohara et al 2002) publish layouts, without detailing cartographic technical explanations. Hence, technical novelty of this work consists in explanation of the GMT workflow using following modules: trend1d, grdcut, makecpt, grdimage, psscale, grdcontour, psbasemap, psxy, grdtrack, convert, pstext, logo, psconvert, as well as Unix echo utility.

Practical approach and theoretical methodology of GMT used for geophysical modelling has many potential applications in further research. They include estimation and specification testing of slope steepness and gradient for analysis of the submarine shape landforms, visualization of the geophysical settings, geological mapping. For example, GMT based cartographic data modelling is applicable to seismic studies of the target areas as well as 2D and 3D models.

Current study presented a developed GMT based approach of the cartographic visualization based on the retrieved geoinformation from raster grids and analysis of the geophysical settings and submarine geomorphology of the trench. Benefits of the methodology consist in the GMT approach and suggested multi-source datasets (ETOPO, EGM96, DEM, NOAA and GSHHGD). Quality of the used datasets are tested and recommended for further applications in marine geology. Possible combinations of the correlation of bathymetry with geological settings are identified in geographical space. Such a model combining programming approach of shell scripting with geological data analysis allows numerical study of similar oceanic trenches assessed based on their tectonic historical development, geological settings and seismicity in space and time. Hence, this paper proposes a new approach for the submarine geomorphic modelling and generating cross-section profiles based on the GMT that integrates geospatial modelling approach and geological analysis within a multi-source project. The principles underlying presented methods of cartographic data analysis are derived from GMT scripting.

Scripting methodology presents several benefits over traditional GIS mapping. The process of the digitizing cross-section profiles was automated using GMT routines by 'grdtrack'. Large numbers of profiles in similar research investigating oceanic trenches can be processed quickly with minimal human intervention. Perceived geometric accuracy can be modeled, visualized and compared to geological and geophysical maps, and the correlation of data assessed. Automated digitizing by 'grdtrack' module eliminates human subjectivity and significantly reduces time needed to produce an interpreted map, which is crucial for long trenches with complicated axis geometry.

6 CONCLUSION

Understanding structure of the submarine landforms of the hadal trenches as the deepest places on the Earth helps to improve investigations of the marine geology and submarine geomorphology of the oceans. Applying spatial analysis for the geo-marine data analysis and processing, using advanced mapping and modelling modules of GMT enables to make deeper insights in to the least accessible part of the Earth: the deep-sea trenches. This research presented successful application of the scripting toolset GMT for marine geology which resulted in high quality precise mapping, fine cartographic instruments, flexibility of the scripting and coding, applicability of the UNIX utilities. Using such advantages of the GMT for geospatial data modelling definitely facilitates data processing, enables detailed analysis and mapping of the oceanographic data sets. As demonstrated, the application of the GMT workflow towards cartographic tasks, geological data analysis and visualization is highly effective and promising comparing to the traditionally used GIS software, because every line code within the shell script is 'responsible' for the visualized layer and can be flexibly changed and adjusted through coding.

Correct cartographic visualization is the key step towards proper understanding and detecting environmental factors in complex systems, such as geology, bathymetry, oceanography, tectonics. Therefore, precise mapping demonstrated by means of the GMT is strongly recommended for further application on marine geological studies. This can specifically be applied for analysis of the structure and functional features of the remotely located objects, such as hadal trenches. Advanced cartographic possibilities presented by GMT toolset results in high quality mapping by various techniques: diverse projections, color palette tables, location of the directional roses, selecting correct fonts and grid lines, illumination of the grids, etc. The results presented as a series of the thematic layers show geological and geophysical phenomena of the study area.

Current paper contributed both towards the marine geological studies and GIS technical development through demonstration of the advanced cartographic solutions by GMT with a case study of Guatemala Trench modelling. High precision cartography, machine learning techniques and scripting flexibility ensure high cartographic standards and suitability of GMT for geological modelling. Main tasks included developed technical methodology of the GMT script used for geological data analysis. These included geophysical modelling, digitizing cross-section profiles, visualizing and analysis of the data sets (gravity and topography surface modelling), 3D-mesh modelling, contour plotting, descriptive statistics. Analysis and visualization of the datasets enabled to map remotely located areas with example of the Guatemala Trench and to map geophysical and geological factors of the study area.

ACKNOWLEDGEMENTS

This document is the results of the research project funded by the China Scholarship Council (CSC) SOA, Marine Scholarship of China, Grant Nr. 2016SOA002, at OUC, Qingdao, P.R.C.

Alvarez Gómez, J. A., Gutiérrez Gutiérrez, O. Q., Aniel-Quiroga, I. N., and González, M. (2012). Tsunamigenic potential of outer-rise normal faults at the Middle America trench in Central America, *Tectonophysics*, **574–575**, 133–143.

Alvarez Gómez, J. A., Meijer, P. T., Martínez- Díaz, J. J., and Capote, R. (2008). Constraints from finite element modeling on the active tectonics of northern Central America and the Middle America Trench, *Tectonics*, **27**, 1–12.

Amante, C., and Eakins, B. W. (2009). *ETOPO1 1 arc-minute Global Relief Model: Procedures, Data Sources and Analysis*. NOAA.

Aubouin, J., Azéma, J., Carfantan, J. C., Demant, A., Rangin, C., Tardy, M., and Tournon, J. (1982). The Middle America Trench in the Geological Framework of Central America, *Deep Sea Drilling Project Reports and Publications*, **67**, 747–755.

Azéma, J., and Tournon, J. (1982). The Guatemalan Margin, the Nicoya Complex, and the Origin of the Caribbean Plate, *Deep Sea Drilling Project Reports and Publications*, **40**, 739–745.

Becker, J. J., Sandwell, D. T., Smith, W. H. F., Braud, J., Binder, B., Depner, J., ... Weather- all, P. (2009, 11). Global bathymetry and elevation data at 30 arc seconds resolution: SRTM30 PLUS, *Marine Geodesy*, **32**, 355–371.

Coulbourn, W. T. (1982). Stratigraphy and Structures of the Middle America Trench, *Deep Sea Drilling Project Reports and Publications*, **67**, 691–706.

Cowan, D. S. (1982). Origin of "Vein Structure" in Slope Sediments on the Inner Slope of the Middle America Trench off Guatemala, *Deep Sea Drilling Project Reports and Publications*, **32**, 645–650.

Dmitriev, Y. I. (1982). Basalts of the Middle America Trench (Guatemala Transect) and Their Correlation With Oceanic and Island-Arc Tholeiites, *Deep Sea Drilling Project Reports and Publications*, **67**, 577–584.

Faas, R. W. (1982). Gravitational Compaction Patterns Determined from Sediment Cores Recovered during the Deep Sea Drilling Project Leg 67 Guatemalan Transect: Continental Slope, Middle America Trench, and Cocos Plate, *Deep Sea Drilling Project Reports and Publications*, **30**, 617–638.

Galli, C. (1979). Ophiolite and island-arc volcanism in Costa Rica, *Geol. Soc. Am. Bull.*, **90**, 444-452.

Gauger, S., Kuhn, G., Gohl, K., Feigl, T., Lemenkova, P. and Hillenbrand, C. (2007). Swath-bathymetric mapping. *Reports on Polar and Marine Research*, **557**, 38–45.

Guzmán-Speziale, M. and Gómez-González, J. M. (2006). Seismic strain rate along the Middle America Trench reveals significant differences between Cocos-North America and Cocos-Caribbean convergence, *Geophysical Journal International*, **166**, 179–185.

Heezen, B. C., and Tharp, M. (1977). *World Ocean Floor Panorama*. New York, U. S.

Huber, P. J. (1964). Robust estimation of a location parameter, *Annals of Mathematical Statistics*, **35**, 73–101.

Huene, R. V., Ladd, J., and Norton, I. (1982). Geophysical Observations of Slope Deposits, Middle America Trench off Guatemala, *Deep Sea Drilling Project Reports and Publications*, **38**, 719–732.

IHO. (2012). *GEBCO Gazetteer of Undersea Feature Names*. IHO-IOC.

Joron, J.-L., Bougault, H., Maury, R. C., and Stephan, J.-F. (1982). Basalt from the Cocos Plate, Site 487, Leg 66: Petrology and Geochemistry, *Deep Sea Drilling Project Reports and Publications*, **66**, 731–734.

Klaučo, M., Gregorová, B., Stankov, U., Marković, V. and Lemenkova, P. (2017). Land planning as a support for sustainable development based on tourism: A case study of Slovak Rural Region, *Environmental Engineering and Management Journal*, **2**(16), 449-458.

Klaučo, M., Gregorová, B., Stankov, U., Marković, V. and Lemenkova, P. (2013a). Determination of ecological significance based on geostatistical assessment: a case study from the Slovak Natura 2000 protected area. Central European Journal of Geosciences 5(1): 28-42.

Klaučo, M., Gregorová, B., Stankov, U., Marković, V. and Lemenkova, P. (2013b). Interpretation of Landscape Values, Typology and Quality Using Methods of Spatial Metrics for Ecological Planning. *54th International Conference Environmental and Climate Technologies*, Riga Technical University, 14 October 2014, Riga, Latvia.

Kuhn, G., Hass, C., Kober, M., Petitat, M., Feigl, T., Hillenbrand, C.-D., Kruger, S., ... Lemenkova P., (2006). The response of quaternary climatic cycles in the South-East Pacific: development of the opal belt and dynamics behavior of the West Antarctic ice sheet. In: Gohl, K. (ed) *Expeditionsprogramm Nr. 75 ANT XXIII/4*, AWI, Bremerhaven, Germany.

Kurnosov, V., Murdmaa, I., Kazakova, V., Mikhina, V., and Shevchenko, A. (1982). Mineralogy of Sediments from the Middle America Trench (Guatemala Transect), *Deep Sea Drilling Project Reports and Publications*, **67**, 515–528.

Kurnosov, V. B., & Shevchenko, A. Y. (1982). Secondary Minerals in Basalts from the Middle America Trench, Leg 67, *Deep Sea Drilling Project Reports and Publications*, **22**, 551–555.

Lemenkova, P. (2011). *Seagrass Mapping and Monitoring Along the Coasts of Crete, Greece*, M.Sc. Thesis. Netherands, University of Twente, 1-158.

Lemenkova, P., Promper, C. and Glade, T. (2012). Economic Assessment of Landslide Risk for the Waidhofen a.d. Ybbs Region, Alpine Foreland, Lower Austria. In Eberhardt, E. et al (Eds.), *Protecting Society through Improved Understanding. 11th Int'l Symposium on Landslides & the 2nd North American Symposium on Landslides & Engineered Slopes. NASL, June 2–8, 2012. Banff, AB, Canada*, 279–285.

Lemenkova, P. (2018a). Factor Analysis by R Programming to Assess Variability Among Environmental Determinants of the Mariana Trench, *Turkish Journal of Maritime and Marine Sciences*, **4**, 146–155.

Lemenkova, P. (2018b). R scripting libraries for comparative analysis of the correlation methods to identify factors affecting Mariana Trench formation, *Journal of Marine Technology and Environment*, **2**, 35–42.

Lemenkova, P. (2019a). Processing oceanographic data by Python libraries NumPy, SciPy and Pandas, *Aquatic Research*, **2**, 73–91.

Lemenkova, P. (2019b). Testing Linear Regressions by StatsModel Library of Python for Oceanological Data Interpretation, *Aquatic Sciences and Engineering*, **34**, 51-60.

Lemenkova, P. (2019c). Numerical Data Modelling and Classification in Marine Geology by the SPSS Statistics, *International Journal of Engineering Technologies*, **5**(2), 90-99.

Lemenkova, P. (2019d). Regression Models by Gretl and R Statistical Packages for Data Analysis in Marine Geology, *International Journal of Environmental Trends*, **3**(1), 39-59.
Lemenkova, P. (2019e). K-means Clustering in R Libraries {cluster} and {factoextra} for Grouping Oceanographic Data, *International Journal of Informatics and Applied Mathematics*, **2**(1), 1-26.
Lemenkova, P. (2019f). Plotting Ternary Diagrams by R Library ggtern for Geological Modelling, *Eastern Anatolian Journal of Science,* **5**(2), 16–25.
Lemenkova, P. (2019g). Statistical Analysis of the Mariana Trench Geomorphology Using R Programming Language, *Geodesy and Cartography*, 45(2), 57–84.
Lemenkova, P. (2019h) GMT Based Comparative Analysis and Geomorphological Mapping of the Kermadec and Tonga Trenches, Southwest Pacific Ocean. *Geographia Technica*, **14**(2), 39-48.
Lyon-Caen, H., Barrier, E., Lasserre, C., Franco, A., Arzu, I., Chiquin, L., . . . Wolf, R. (2006). Kinematics of the North American-Caribbean-Cocos plates in Central America from new GPS measurements across the Polochic-Motagua fault system, *Geoph. Res. Let.*, **33**, 1–5.
Menke, W. (1989). *Geophysical Data Analysis: Discrete Inverse Theory.* Rev. Ed., Academic Press, San Diego.
Monahan, D. (2004). GEBCO: the Second Century, *Hydro International*, **8**, 1-10.
Moore, G., Lonsdale, P., & Huene, R. v. (1982). Near-Bottom Observations of the Middle America Trench off Guatemala, *Deep Sea Drilling Project Reports and Publications,* **67**, 707–718.
Ohara, Y., Fujioka, K., Ishizuka, O., & Ishii, T. (2002). Peridotites and volcanics from the Yap arc system: implications for tectonics of the southern Philippine Sea Plate, *Chemical Geology*, **189**, 35–53.
Rew, R. K., and Davis, G. P. (1990). NetCDF: an interface for scientific data access, *IEEE Computer Graphics and Applications*, **10**, 76–82.
Ross, D. A. (1971). Sediments of the northern Middle America Trench, *Geological Society of America Bulletin*, **82**, 303–322.
Ross, D. A., and Shor, G. G. (1965). Reflection profiles across the Middle America Trench, *Journal of Geophysical Research Atmospheres,* **70**, 5551-5572.
Sandwell, D. T., Garcia, E., Soofi, K., Wessel, P., and Smith, W. H. F. (2013). Towards 1 mGal Global Marine Gravity from CryoSat-2, Envisat, and Jason-1, *The Leading Edge*, **32**, 892–899.
Sandwell, D. T., Müller, R. D., Smith, W. H. F., Garcia, E., and Francis, R. (2014). New global marine gravity model from CryoSat-2 and Jason-1 reveals buried tectonic structure, *Science*, **346**, 65–67.
Sandwell, D. T., Yale, M. M., and Smith, W. H. F. (1997). Marine gravity anomalies from GEOSAT and ERS-1 satellite altimetry, *J. of Geophys Res. Atm*., **102**, 10039–10054.
Schenke, H. W. and Lemenkova, P. (2008). Zur Frage der Meeresboden-Kartographie: Die Nutzung von AutoTrace Digitizer für die Vektorisierung der Bathymetrischen Daten in der Petschora-See. *Hydrographische Nachrichten*, **25**(81), 16–21.
Schmidt-Effing, R. (1979). Alter und Genese des Nicoya-Komplexes, einer ozeanischen P`alaokruste (Oberjura bis Eoz`an) im sudlichen Zentralamerika, *Geologische Rundschau*, **68**, 457–494.
Shepard, F. P. (1963). *Submarine Geology*. New York, U.S.: Harper & Row.
Shipboard Scientific Party. (1982a). Site 498: Middle America Trench Lower Slope, *Deep Sea Drilling Project Reports and Publications*, **6**, 245–266.
Shipboard Scientific Party. (1982b). Site 495: Cocos Plate – Middle America Trench Outer Slope, *Deep Sea Drilling Project Reports and Publications*, **1**, 79–141.
Shipboard Scientific Party. (1982c). Site 496: Middle America Trench Upper Slope, *Deep Sea Drilling Project Reports and Publications*, **4**, 143–192.
Shipboard Scientific Party. (1982d). Site 499: Middle America Trench Axis, *Deep Sea Drilling Project Reports and Publications*, **7**, 267–314.
Shipboard Scientific Party. (1982e). Site 500: Middle America Trench Axis, *Deep Sea Drilling Project Reports and Publications*, **8**, 315–347.

Smith, W. H. F. (1993). On the accuracy of digital bathymetric data, *J. Geoph. Res.*, **98**, 9591–9603.
Smith, W. H. F., and Sandwell, D. T. (1995). Marine gravity field from declassified Geosat and ERS-1 altimetry, *EOS Trans. Am. Geophys. Un*., **76**, 1–10. (Fall Mtng Suppl, F156)
Smith, W. H. F., and Sandwell, D. T. (1997b). Marine gravity field from declassified Geosat and ERS-1 altimetry, *J. Geophys. Res.* **102**, 10039–10054.
Suetova, I. A., Ushakova, L. A. and Lemenkova, P. (2005a), Geoinformation mapping of the Barents and Pechora Seas, Geography and Natural Resources, 4, 138-142.
Suetova, I., Ushakova, L. and Lemenkova, P. (2005b), Geoecological Mapping of the Barents Sea Using GIS. In: Digital Cartography, GIS for Sustainable Development of Territories. *Proceedings of the International Cartographic Conference, July 9-16 2005*, La Coruña, Spain.
Turcotte, D. L., and Schubert, G. (2013). *Geodynamics* (2nd ed.). U.K.: Cambridge University Press.
Wessel, P., and Smith, W. H. F. (1996). A Global Self-consistent, Hierarchical, High-resolution Shoreline Database, *J. Geophys. Res.*, **101**, 8741–8743.
Wessel, P., and Watts, A. B. (1988). On the accuracy of marine gravity measurements, *Journal of Geophysical Research*, **93**, 393–413.